J Mater Sci: Mater Med (2009) 20:1419–1426
DOI 10.1007/s10856-009-3708-2

Nanostructural analysis of trabecular bone

Sun Ig Hong · Soon Ku Hong · David H. Kohn

Received: 17 September 2008 / Accepted: 6 February 2009 / Published online: 6 March 2009

Abstract The mechanical properties of bone are dictated by the size, shape and organization of the mineral and matrix phases at multiple levels of hierarchy. While much is known about structure–function relations at the macroscopic level, less is known at the nanoscale, especially for trabecular bone. In this study, high resolution transmission electron microscopy (HRTEM) was carried out to analyze shape and orientation of apatite crystals in murine femoral trabecular bone. The distribution and orientation of mineral apatites in trabecular bone were different from lamellar bone and the c-axis of the tablet-like mineral apatite crystals in trabecular bone was arranged with no preferred orientation. The difference in the orientation distribution of apatite crystals of trabecular bone in the present study compared with that of lamellar bone found in the literature can be attributed to the more complex local stress state in trabecular bone. Apatite crystals were also found to be multi-crystalline, not single crystalline, from dark field image analysis. From the observations of this study, it is suggested that Wolff's law can be applicable to the nanostructural orientation and distribution of apatite crystals in trabecular bone. It was also found that small round crystalline particles observed adjacent to collagen fibrils were similar in size and shape to the apatite crystals in biomimetically nucleated synthetic amorphous calcium phosphate, which suggests that they are bone mineral apatite nuclei.

S. I. Hong (✉) · D. H. Kohn
Department of Biologic and Materials Sciences,
University of Michigan, Ann Arbor, MI 48109-1078, USA
e-mail: sihong@cnu.ac.kr

S. I. Hong
Department of Nanomaterials Engineering,
Chungnam National University, Taejon 305-764, Korea

S. K. Hong
Department of Materials Science and Engineering,
Chungnam National University, Taejon 305-764, Korea

D. H. Kohn
Department of Biomedical Engineering, University
of Michigan, Ann Arbor, MI 48109-2099, USA

1 Introduction

Bone is one of the most complex building materials of the body and its unique physical and chemical attributes mirror the diversity of its function [1]. The morphology, dimensions and distribution of apatite crystals affect the mechanical properties of bones. Mature crystals are plate shaped and are oriented with the c-axis parallel to the collagen fibrils [2, 3]. While detailed information concerning the morphology, distribution and dimensions of apatite crystals is now available, such data have been obtained mostly from avian tendon and lamellar bone [1–3]. The organization of collagen fibrils differs in different types of bone [4] and it affects the morphology and orientation of the mineral crystals associated with them. For example, apatite crystals in woven bone are also platelet-shaped, but the average crystal dimensions are smaller than those of mature crystals in lamellar bone [4]. There is also less preferential orientation and organization of apatite crystals in woven bone [4] compared with lamellar bone. Trabecular bone is much more porous and does not generally contain vascular channels like cortical bone. The structure of the trabecular bone at the nanostructural level may also be different from that of lamellar bone because the stress state in trabecular bone is different from that of lamellar bone [5–7].

The morphology, distribution and dimensions of apatite crystals in trabecular bone [5, 6] are not as extensively studied as in lamellar bone, and our understanding of the size and orientation distribution of apatite crystals and collagen fibrils in trabecular bone is not as complete. As no detailed studies have been performed on trabecular bone at this level, it is generally presumed that the structure at the nanostructural level, i.e. the collagen and mineral structure is similar to that of cortical bone. Rohanizadeh et al. [5] noted a preferred crystal orientation in the vertebral trabeculae of rat bone. Recently, Rubin et al. [6] found that the lower bone mineral density in osteoporotic human trabecular bone is caused by a reduction in trabecular volume, rather than an alteration of the bone crystals at the nanoscale. However, diffraction analyses for the determination of crystal orientation were not available from their study [6]. In trabecular bone, the arrangement of trabeculae appears to be random, but trabeculae are known to be aligned along the principal stress directions [7]. The alignment of trabeculae with principal stress directions can be explained by the adaptation of bone structure responding to a mechanical stimulus [7]. Since the stress state of trabecular bone is more complex than that of the lamellar bone [7], the arrangement of the apatite crystals may be different from that in lamellar bone. Nevertheless, the orientation of apatite in trabecular bone has not been investigated as thoroughly compared to that of lamellar bone. The objectives of the present research therefore were to examine the ultrastructure of murine trabecular bone, analyzing the shape and orientation of apatite crystals through high resolution image and diffraction pattern analyses. The size, shape and orientation distribution of apatite crystals determined in the present study are also compared with those of lamellar bone found in the literature [2, 3, 7, 8] and the applicability of the Wolff's law [7] in trabecular bone at the nanoscale is examined.

2 Materials and methods

Femora were harvested from male C57BL6 mice ($n = 5$) aged 8 months. The soft tissue was carefully dissected and the proximal femur was sectioned off with a low speed saw with calcium buffered saline solution as a lubricant and coolant. Specimens were fixed in Sorenson's buffer with 2.5% glutaraldehyde, postfixed in 1% osmium tetroxide and dehydrated in an ethanol series (30, 50, 70, 90, 100%) and acetone (100%). Specimens were next infiltrated with a series of graded mixtures of acetone and Spurr resin (Ted Pella, Redding, CA; prepared with epoxy monomer vinyl cyclohexene (ERL), diglycidyl ether of polypropylene glycol (DER 736), nonenyl succinicanhydride and dimethylaminoethanol (DMAE)) and embedded in fresh Spurr resin in Beem embedding capsules. Embedded samples were polymerized at 65°C for 24 h. Ultrathin sections (60–70 nm) were cut perpendicular to the axis of the long bone with a diamond knife on a MIL ultramicrotome and picked up on 300-mesh Cu grids.

Since the axis of each trabeculae is not necessarily parallel to the bone axis, and in some cases even perpendicular as shown in Fig. 1 [5], only macroscopically transverse sections were observed in this study. However, both transverse and longitudinal sections of individual trabeculae were observed under the TEM to analyze the ultrastructure of trabeculae of different orientations. Figure 1 shows the variation in trabecular orientation of an

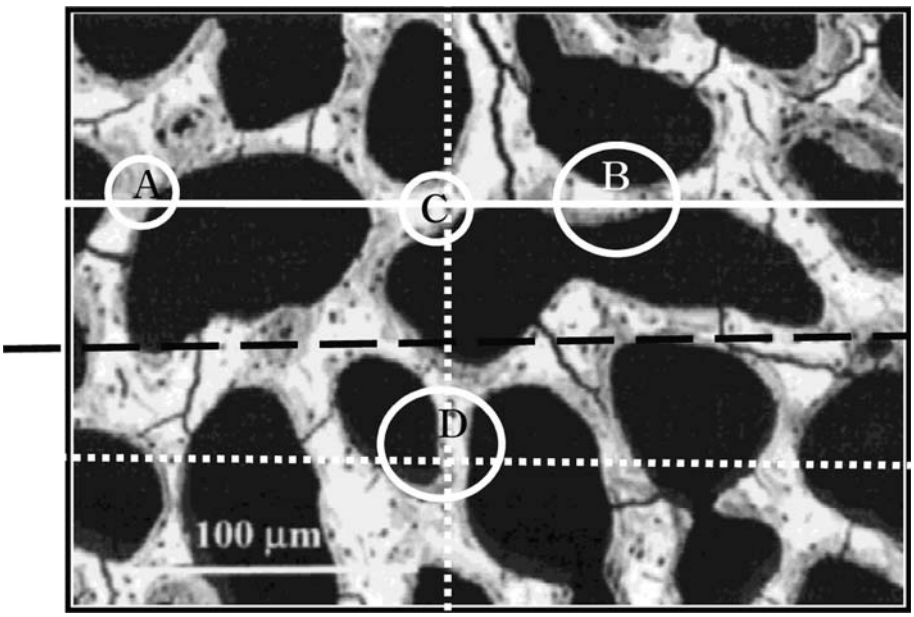

Fig. 1 Variation in trabecular orientation in extracted areas of trabecular bone. Orientation is dependent on the location of TEM sections, but both longitudinal and transverse trabeculae can be obtained from a macroscopically transverse section. SEM image of trabecular bone from [5]. Courtesy of R. Rohanizadeh

extracted area of trabecular bone similar to that used in the TEM analyses. Trabecular orientation is dependent on the location at which sections were made. The scanning electron microscopy (SEM) image is shown to explain the effect of the sectioning location on the orientation of the structure. In this figure, if the TEM thin sections were cut along the white straight line, the region "A" would reveal the transverse section of trabeculae whereas the region "B" would reveal the longitudinal section of trabeculae. Likewise, a thin section along the black dashed line would show mostly the longitudinal section of trabeculae and a thin section along the white dotted horizontal line would show mostly the transverse section of trabeculae. A section along the vertical dotted line would also reveal either a transverse (region "C") or longitudinal section (region "D") of the trabeculae, depending on the location.

Twelve Cu grids with five ultra thin sections collected in each grid were prepared and observed. Thin sections were randomly collected from various regions and both longitudinal and transverse sections of trabeculae were included in thin sections. Since we can't pinpoint orientation of trabeculae during sectioning, we assume we have a range of orientations in our TEM samples. The equivalent nanostructures observed throughout this range of sections imply no orientation effects. Therefore, it can be reasonably assumed that the observations in this study represent the average nano-structure of the trabecular bone irrespective of the local orientation of the trabeculae.

High resolution transmission electron microscope (HRTEM) observations were carried out using a JEOL JEM2010 (Tokyo, Japan) electron microscope operated at 200 kV. In order to determine the crystal structure of the mineral phase, selected area electron diffraction (SAED) was performed. For analyses of HRTEM images, the observed electron micrographs were digitized with 256 gray levels and 512 × 512 pixels from photographic films using a computer-aided image processor. Using the digitized data, fast Fourier transform (FFT) patterns with noise filtering were analyzed.

3 Experimental results

Mineralized collagen fibrils with tablet-like crystals, interpreted as an edge view of plate-like crystals observed by others [6] were observed (Fig. 2a). The dark and dense phases indicated by arrows are apatite crystals [5, 6, 8, 9] and gray fibers are collagen fibrils [9]. Collagen fibrils and needle-like apatite crystallites have a similar morphology, which can be distinguished by diffraction technique, energy dispersive X-ray spectroscopy (EDX), and HRTEM observations [9]. Apatite crystallites always give out crystalline diffraction spots, and are stable enough for HRTEM observation, whereas collagen fibrils are unstable and prone to contamination by an electron beam. The length of the apatite crystals was 46.2 ± 13.8 nm. A relatively smooth and continuous diffraction ring of (002) planes was noted in this area (Fig. 2b). The presence of the (002) ring indicates that the c-axis of the tablet-like mineral apatite crystals was arranged with no preferred orientation in the plane of the image. The relatively random orientation distribution of collagen fibrils and crystals in Fig. 2a is compatible with the presence of a relatively continuous (002) diffraction ring since the c-axes of the crystals are roughly parallel to the long axes of the collagen fibrils [2]. One interesting observation is the presence of the weak partial (120) ring, suggesting that the c-axes of some crystals are perpendicular to the plane of the view in Fig. 2a, since the (120) plane is perpendicular to the (002) plane.

Mineral crystals with (002) and (121) lattice fringes were most frequently observed, consistent with the high intensities of the (002) and (121) rings in Fig. 2b. Figure 3a and b show HRTEM images of tablet-like crystals with (002) and (121) lattice fringes, respectively. In these

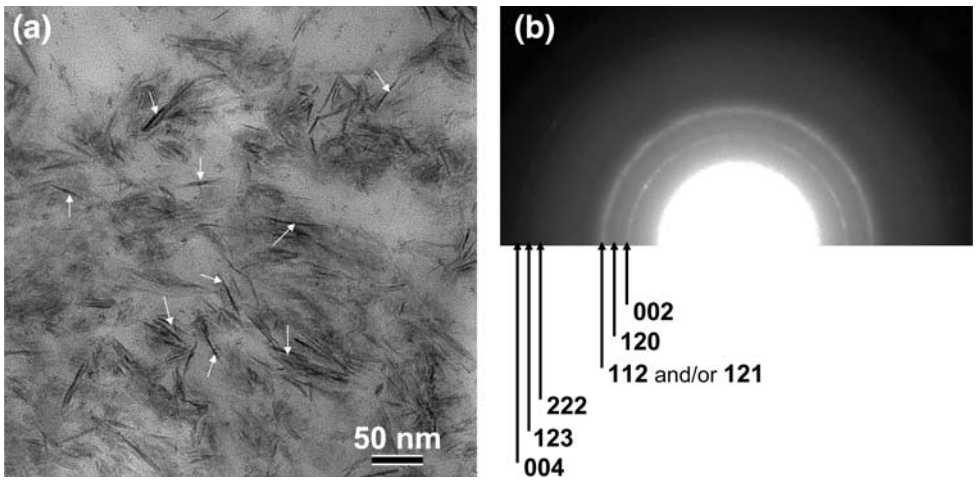

Fig. 2 TEM image (**a**) of collagen fibrils and apatite crystals (some crystals indicated by *arrows*) and diffraction pattern (**b**) from the ~500 × 500 nm^2 area of the view in (**a**). The length of the apatite crystals was 46.2 ± 13.8 nm. A relatively smooth and continuous diffraction ring of (002) planes was noted in this area. The presence of the continuous (002) ring indicates that the c-axis of the crystals has no preferred orientation

figures, lattice fringes of the (002) and (121) planes are indicated by two parallel lines in squares delineated by broken lines. The spacing between (002) and (121) planes was 0.344 nm and 0.281 nm respectively (the spacing was determined by the linear intercept method by counting the lattice fringes along a line perpendicular to the lattice fringe line). The fast Fourier transformation (FFT) image (Fig. 4a) and the inverse fast Fourier transformation (IFFT) pattern (Fig. 4b) obtained from the area enclosed by the square in Fig. 3a show that the zone axis (Z) of the lattice fringes in Fig. 3a was [100], meaning the plane of view for the crystals in this area is (100), which is perpendicular to c-axis of apatite.

Figure 5 shows bright (a) and dark (b, c) field images of the same area (denoted by white arrows) of a specimen, taken from the parts of the diffraction rings marked with a circle in Fig. 5b and c where the aperture was placed. Dark field images in Fig. 5(b) and 5(c) were obtained by placing the objective aperture on the small fraction of the (112) and (004) rings, respectively (see Fig. 2 for identification of rings). The length of apatite crystals highlighted in the dark field images is 5–10 nm in Fig. 5b, compared to the 46.2 nm average length of apatite crystals in the bright field images in Figs. 2 and 5a, suggesting that only a fraction of the crystals is highlighted in Fig. 5. This observation suggests that the orientation of each apatite mineral is not the same throughout the crystal and contains a low angle boundary.

Numerous small round darker particles were observed adjacent to the collagen fibrils (Fig. 6a). A HRTEM image of the small round particles at a higher magnification (Fig. 6b) shows that the size of particles was 1.83 ± 0.26 nm and the spacing of the lattice fringes in each particle was approximately 0.28 nm. This type of round particle has been observed by others [10], but lattice fringes have not been reported, probably because the fringes with 0.28 nm spacing are too small to be easily detected in thin sections [1].

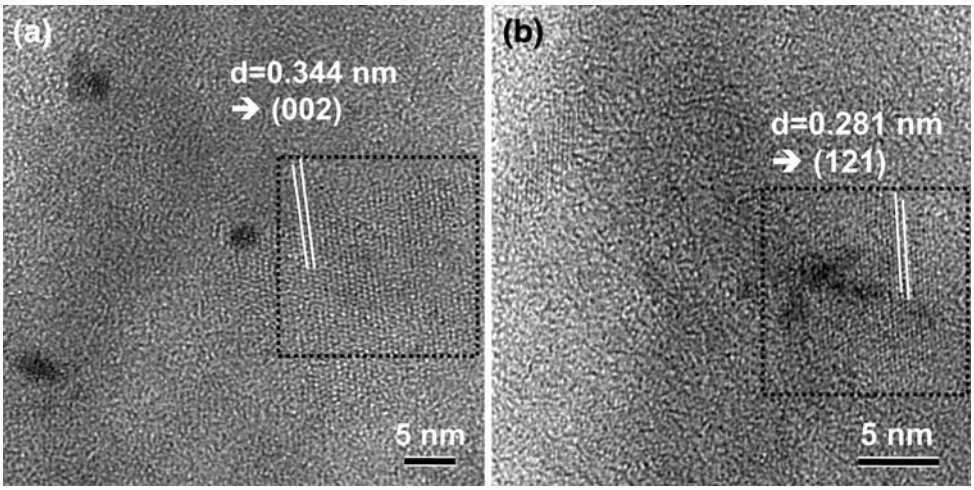

Fig. 3 TEM images of tablet-like crystals with (002) lattice fringes (**a**) and (121) lattice fringes (**b**). Mineral crystals with (002) and (121) lattice fringes were most frequently observed, consistent with the high intensities of (002) and (121) rings in Fig. 1b

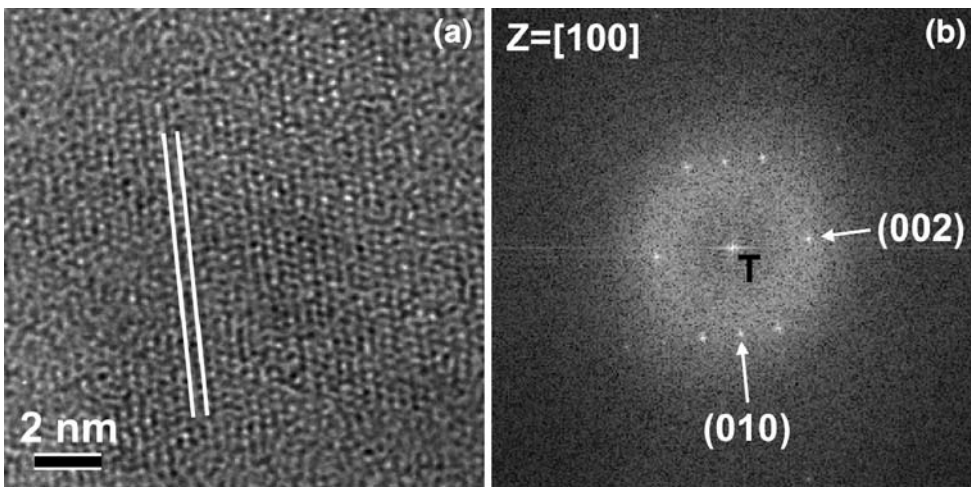

Fig. 4 Fast Fourier transformation (FFT) image (**a**) and inverse fast Fourier transformation (IFFT) pattern (**b**) obtained from the image enclosed by the square delineated by broken lines in Fig. 3a. The zone axis (Z) of lattice fringes is [100], meaning the plane of view for the crystal in Fig. 3a is (100), which is perpendicular to c-axis of apatite

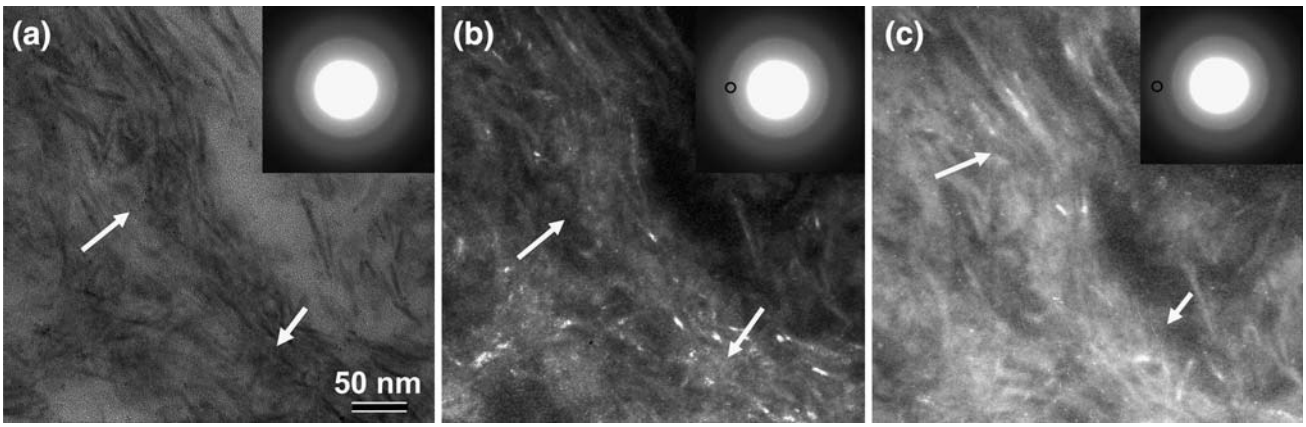

Fig. 5 Bright (**a**) and dark (**b**, **c**) field images of the same area taken from the part of the diffraction rings marked with a small circle in the inset of (**b**) and (**c**) to indicate where the object aperture was placed. (**b**) and (**c**) were obtained from the (112) and (004) rings, respectively (see Fig. 2 for identification of rings). The same location of the specimen is marked with *arrows*

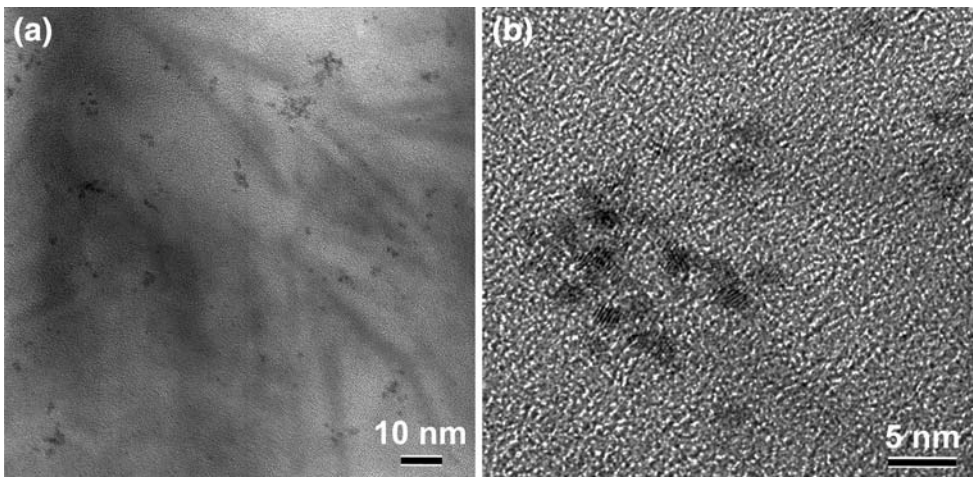

Fig. 6 (**a**) A region with collagen fibrils and small round particles. (**b**) HRTEM image of the small round particles at a higher magnification. Numerous round particles were observed at the tip of collagen fibrils or close to collagen fibril. The size of particles was approximately 2 nm and the spacing of the lattice fringes in each particle was approximately 0.28 nm

4 Discussion

4.1 Orientation of bone mineral

One important observation in the present study of femoral trabecular bone is the arrangement of collagen fibrils and apatite crystals with no preferred orientation (Fig. 2a), as supported by the presence of a continuous (002) diffraction ring (Fig. 2b). Rubin et al. [6] examined trabecular bone without orientation analyses, but the undulated circular arrangement of collagen fibrils suggests no preferred orientation since the apatite crystals are usually parallel to the collagen fibrils. The distribution of collagen fibrils in Fig. 2 appears similar to the radial fibril arrays observed in the bulk of dentin [11]. In dentin, the tubules are surrounded by collagen fibrils that are mostly in one plane, with no preferred orientation (e.g. Fig. 6d of [11]). A wide variation in the length of apatite crystals (46.2 ± 13.8 nm) in this study may have resulted from the arrangement of apatite crystals with no preferred orientation.

On the other hand, a preferred orientation of crystals has been noted in rat vertebral trabecular bone [5]. However, a close examination of the TEM images shows that on a larger scale there are sets of collagen fibrils with different orientations (e.g. Fig. 3 of [5]). This result therefore suggests that the orientation of crystals on a larger scale has no preferred orientation. Our observation of a lack of preferred orientation differs from that of Rohanizadeh et al. [5] because we observed a more uniform and random distribution of crystals on a much smaller scale (for example, compare the diffraction of the present study and that of Rohanizadeh et al. [5]). Another difference is the absence of a partial (120) ring in the result of Rohanizadeh et al. [5], indicative of a locally different orientation distribution of apatite crystals in different trabecular bones.

Synchrotron radiation studies [8] suggest that two groups of crystallite orientations exist in lamellar bone, one parallel to the Haversian system and the other perpendicular. This observation can be attributed to the rotated plywood structure of lamellar bone. The distribution of

collagen fibrils and mineral crystals with no preferred orientation in Fig. 2 is therefore different from that of lamellar bone. A less ordered arrangement of collagen fibrils and thus less preferential orientation and organization of the apatites has also been noted in human woven bone [4] and dentin [11].

The distribution of collagen fibrils and apatite crystals observed in the present study is also similar to the distribution observed in human trabecular bone (e.g. Fig. 2 of [6]). Rubin et al. [6] noted that the crystal organization was random and changed within a 100–200 nm diameter area in a transverse section. In Fig. 2a, the crystal arrangement was observed within an approximately 100 nm diameter. Rubin et al. [6] also observed longitudinal sections of trabecular bone in which apatite crystals were arranged in parallel. Since the tilt axis of each trabeculae varies from region to region and it is known to be aligned along the principal stress direction, it is not certain whether the difference in structure between transversely and longitudinally sectioned trabecular bone in the work of Rubin et al. [6] reflects an orientation difference of the structure, a variation of the structure depending on the local stress state, or some combination of these mechanisms.

Rubin et al. [6] assumed that the c-axis is perpendicular to the plane of their cross sections, but did not carry out diffraction analyses to determine the crystal orientation. However, the similarity in size, shape and distribution of collagen fibrils and mineral crystals between human [6] and murine trabecular bone observed in this study suggests that the c-axis of apatite crystals in the cross-sectional view of human trabecular bone [6] is parallel to the plane of the cross section (e.g. Fig. 2 of [6]). This view on the orientation of the c-axis in human trabecular bone is further supported by the suggestion that apatite crystals are usually formed with the c-axis of crystals oriented parallel to the long axis of the collagen fibril [3, 11–13], and the fact that collagen fibrils were observed to lie mostly in the plane of view. It is not clear, however, how close the orientation and distribution of apatites are between human and murine trabecular bone. The orientation of the c-axis of apatites in trabecular bone can only be determined by local diffraction analysis using TEM or XRD (X-ray diffractometer) and warrants further study.

4.2 Application of Wolff's law to the nanostructure of the trabecular bone

The ultrastructure of trabecular bone contains a variety of apatite crystal orientations, which may reflect a site-specific orientation of apatite crystals. In trabecular bone, the arrangement of trabeculae is aligned along the principal stress directions [7]. The ability of bone to align trabeculae with stress trajectories is accomplished by cells forming and resorbing bone according to variations in functional stimuli [7]. Although the orientation relationship between the trabeculae and the principal stress direction is well established on the micro-scale, the relationship between apatite crystal orientation and principal direction has not been explored. The trabecular bone in the proximal human femur is subjected to a more complex stress state than the lamellar bone in the mid-diaphysis [7, 14] (i.e. more than one principal stress component in some regions [7]). In the region where the major stress components are two or three dimensional, the apatite crystals need to be oriented such that they can resist the load from various directions. The alignment of the apatite crystals may vary locally, leading to site-specific orientation to effectively resist the local stress state. This may explain the random circular arrangement of collagen fibrils and the lack of preferred crystal orientation observed in the trabecular bone in this study and by other investigators [6].

A difficulty involved in the analyses of bone mineral orientation is that the local orientation of trabeculae varies with respect to the global orientation of the trabecular bone from region to region. A question that can be raised is whether the trabeculae which lie perpendicular to the long axis of trabecular bone have a similar micro/nano-structure as the trabeculae parallel to the axis. The analyses in this study are based on the assumption of nanostructural similarity between trabeculae with different orientations, and have some limitations. The distribution and arrangement of mineral and matrix constituents in bone result from external and/or internal loads and the macro- and microstructural alignment of trabeculae lie along the principal directions as proposed in Wolff's law. The same principle can be applied to the nano-structural arrangement of apatite crystals as suggested in this study. More extensive studies on the site-specific nano-structure of the trabeculae, which may require a more accurate and detailed sample sectioning technique than the currently available one, are needed to clarify whether nanostructural similarity of trabeculae exists irrespective of orientation.

4.3 Shape of apatite nuclei

An important observation in the present study is the presence of small round crystalline particles between or adjacent to collagen fibrils (Fig. 6). It is well established that mature apatite crystals are plate-shaped [6]. However, the images of round particles with crystal fringes are a new observation. Early deposits of bone minerals are extremely small (<1 nm) [1] and it is difficult to detect these round crystal particles. The observation of crystal fringes in small round particles was possible because high resolution transmission electron microscopy was used. The size of minerals containing even the smallest recognizable crystals

(1–2 nm) is large in comparison with the theoretically smallest ion clusters (<1 nm) precipitated in the early stage of mineral crystal formation. Accordingly, the understanding of the size, shape and distribution of early nuclei of mineral crystals is still poor.

The shape of a crystal changes with an increase in size in many materials [15, 16]. The interfacial energy and the strain energy are important factors in determining the shape of nuclei [15]. For example, if the coherency strain is negligible, the shape becomes independent of strain energy and a spherical shape which requires minimum interface energy is preferred [15]. In the case of stiff incoherent nuclei precipitated in an isotropic matrix, the plate-shaped precipitates are preferred as they minimize the strain energy [15]. In general, the surface energy plays a greater role with a decrease in size since the interface to volume ratio increases with a decrease in size. The shape of the apatite crystals in the early stage of mineralization may therefore be linked to the interface to volume ratio.

The nucleation mechanism of bone minerals is not well established, possibly because of the difficulty involved in the nanostructural analyses of bone minerals. Most of the studies on the structure of the mineral component of bone were conducted on mature crystals [1–3, 5, 6, 13]. There is a report, however, that the shape of mineral crystals in bones also changes with size. Hohling [10] stated that thin rods developed from dot-like nuclei during mineralization of bone and plate-like crystals with a more highly developed crystallinity formed from the thin rods. This observation has some similarity with the precipitation behavior observed in other materials [16]. For example, needle-shaped precipitates developed from initially nano-sized spherical particles (5 nm) in Al–Mg–Si alloy based composites [16]. The dot-like nuclei observed by Hohling [10] in the initial stage of mineralization may therefore be linked to the round crystalline particles observed in this study (Fig. 6).

The possibility of false images resulting from artifacts was carefully examined and excluded for the following reasons; first, the spacing between fringes in round particles is approximately 0.27–0.29 nm, which is close to the spacing of (112) planes of hydroxyapatites (0.278 nm) [13, 17]. Second, the misorientation angles between adjacent particles is very low (as evidenced by approximately parallel lattice fringes in adjacent particles), suggesting that the orientation of nuclei is somewhat controlled by the substrate. It is well known that the c-axis of apatites and the helical axis of the collagen molecules have strongly preferred orientations [18]. Third, the small round particles observed in trabecular bone (Fig. 6b) are similar, in size and shape, to the hydroxyapatite crystals nucleated in vitro from amorphous calcium phosphate [17, 19]. The similarities in the overall size, shape and spacing of lattice fringes between small round crystalline particles in trabecular bone and small crystalline particles in biomimetically nucleated calcium phosphate supports that the observed small round particles are mineral apatite nuclei.

4.4 Nature of the bone mineral crystal

The observation that only part of the apatite crystals was highlighted in the dark field image (Fig. 5) suggests that the orientation of crystals changes even in single apatite plates and, therefore, bone mineral crystals are not single crystalline, but multi-crystalline with low angle grain boundary. This observation is compatible with the suggestion of Landis et al. [2] that crystals in local regions of collagen form by independent nucleation processes. The formation of a large platelet by joining independent nuclei may have resulted in the multi-crystalline crystal if each nuclei were not nucleated with the same orientation. Cuisinier et al. [20] observed bi-crystalline mineral apatites with a misorientation angle of 4^{o} in a chicken tibial bone. The low misorientation angle between grains indicates that nanometer-sized nuclei were nucleated under the influence of the collagen fibrils although they were not oriented the same by the collagen substrate. The observation of a multi-crystalline nature of apatites suggests that multi-crystallinity is a general phenomenon in bone mineral apatites. The growth and joining of adjacent apatite nuclei with slight misorientations (Fig. 6b) appears to have resulted in multi-crystalline apatite minerals.

In summary, we have observed that the distribution and orientation of mineral apatites in murine trabecular bone are different from those typically observed in lamellar bone, and are associated with the more complex local stress state in trabecular bone. From the observations of this study, it is suggested that Wolff's law can be applicable to the nanostructural orientation and distribution of apatite crystals in trabecular bone. We also observed crystalline images of small round nuclei near the collagen fibrils for the first time, and multi-crystallinity of apatites. The results of the present study provide insight into the orientation distribution of apatite crystals in trabecular bone and the nature of apatite nuclei and mature crystals in general, and may help understand mechanical properties at the nanoscale.

Acknowledgment We acknowledge the support from US DoD/Dept. of the Army DAMD17-03-1-0556. SIH is grateful for the support from Korea Research Foundation (D00318).

References

1. Hancox NM. Biology of bone. Cambridge: Cambridge University Press; 1972. p. 3–48.

2. Landis WJ, Song MJ, Leith A, McEwen L, McEwen BF. Mineral and organic interaction in normally calcifying tendon visualized in three dimensions by high voltage electron microscopic tomography and graphic imaging reconstruction. J Struct Biol. 1993;110:39–54. doi:10.1006/jsbi.1993.1003.
3. Rho JY, Kuhn-Spearing L, Zioupos P. Mechanical properties and the hierarchial structure of bone. Med Eng Phys. 1998;20:92–102.
4. Su X, Sun K, Cui FZ, Landis WJ. Organization of apatite crystals in human woven bone. Bone. 2003;32:150–62.
5. Rohanizadeh R, LeGeros RZ, Bohie S, Pilet P, Barbier A, Daculsi G. Ultrastructural properties of bone mineral of control and ti-ludronate-treated osteoporotic rat. Calcif Tissue Int. 2000;67:330–6. doi:10.1007/s002230001141.
6. Rubin MA, Jasiuk I, Taylor J, Rubin J, Ganey T, Apkarian RP. TEM analysis of the nanostructure of normal and osteoporotic human trabecular bone. Bone. 2003;33:270–82. doi:10.1016/S8756-3282(03)00194-7.
7. Martin RB, Burr DB, Sharkey NA. Skeletal tissue mechanics. New York: Springer; 1998. p. 227–30.
8. Rindby A, Voglis P, Engstrom P. Microdiffraction studies of bone tissues using synchrotron radiation. Biomaterials. 1998;19:2083–92. doi:10.1016/S0142-9612(98)00120-3.
9. Chen QZ, Wong CT, Lu WW, Cheung KMC, Leong JCY, Luk KDK. Strengthening mechanism of bone bonding to crystalline hydroxyapatite in vivo. Biomaterials. 2004;25:4234–54. doi:10.1016/j.biomaterials.2003.11.017.
10. Hohling HJ. Collagen mineralization in bone, dentine, cementum and cartilage. Naturwissenschaften. 1969;56:466–76. doi:10.1007/BF00601080.
11. Weiner S, Wagner HD. The material bone: structure-mechanical function relations. Annu Rev Mater Sci. 1998;28:271–98. doi:10.1146/annurev.matsci.28.1.271.
12. Landis WJ. The strength of a calcified tissue depends in part on the molecular structure and organization of its constituent mineral crystals in their organic matrix. Bone. 1995;16:533–44. doi:10.1016/8756-3282(95)00076-P.
13. Sahar ND, Hong SI, Kohn DH. Micro- and nano-structural analyses in bone. Micron. 2005;36:617–29. doi:10.1016/j.micron.2005.07.006.
14. Khan K, McKay H, Kannus P, Bailey D, Wark J, Bennel K. Physical activity and bone health. Champaign: Human Kinetics; 2001. p. 16.
15. Jena AK, Chaturvedi MC. Phase transformation in materials. Englewood Cliffs: Prentice Hall; 1992. p. 151, 302.
16. Hong SI, Gray GT, Wang Z. Microstructure and stress-strain response of Al-Mg-Si alloy composites reinforced with 15% Al_2O_3. Mater Sci Eng. 1996;221:38–47. doi:10.1016/S0921-5093(96)10483-4.
17. Hong SI, Lee KH, Outslay M, Kohn DH. Ultrastructural analyses of nanoscale apatite biomimetically grown on organic template. J Mater Res. 2008;23:478–85. doi:10.1557/jmr.2008.0051.
18. Sasaki N, Sudoh Y. X-ray pole figure analysis of apatite crystals and collagen molecules in bone. Calcif Tissue Int. 1997;60:361–7. doi:10.1007/s002239900244.
19. Luong LN, Hong SI, Patel RJ, Outslay ME, Kohn DH. Spatial control of protein within biomimetically nucleated mineral. Biomaterials. 2006;27:1175–84. doi:10.1016/j.biomaterials.2005.07.043.
20. Cuisinier FJG, Steuer P, Brisson A, Voegel JC. High resolution electron microscopy of crystal growth mechanisms in chicken bone composites. J Cryst Growth. 1995;156:443–53. doi:10.1016/0022-0248(95)00237-5.